Inorganic Chemistry

Article

pubs.acs.org/IC

2,2′-Bipyridine Compounds of Group 14 Elements: A Density Functional Theory Study

Jason England and Karl Wieghardt*

Max Planck Institute for Chemical Energy Conversion, Stiftstrasse 34-36, D-45470 Mülheim an der Ruhr, Germany

Supporting Information

ABSTRACT: The molecular and electronic structures of the 2,2′-bipyridine containing series of group 14 compounds (a) $[MF_4(bpy)]^0$; (b) $[MCl_2(bpy)_2]^{2+/0}$ (c) $[MCl_2(bpy)]^0$; (d) $[M(bpy)_2]^{2+/0}$; (e) $[Si(bpy)_3]^{1+,0,1-,2-}$; and (f) $[M(bpy)_3]^0$ (M = C, Si, Ge, Sn, Pb) have been calculated using density functional theory (DFT). Where possible, geometry optimized structures are compared with their experimentally determined structures. In general, good to excellent agreement is observed. It is shown that the three successive one-electron reductions within the experimentally known series $[Si(bpy)_3]^{1+,0,1-,2-}$ are ligand-based and the Si center has a +IV oxidation state throughout. Hence, these species have the electronic structures $[Si^{IV}(bpy^{\bullet})_3]^+$ (S = 1/2), $[Si^{IV}(bpy^{\bullet})_2(bpy^{2-})]^0$ (S = 0), $[Si^{IV}(bpy^{\bullet})(bpy^{2-})_2]^-$ (S = 1/2), and $[Si^{IV}(bpy^{2-})_3]^{2-}$ (S = 0). Similarly, it is shown that the crystallographically characterized compound $[Si(bpy)_2]^0$ (S = 0) possesses the electronic structure $[Si^{IV}(bpy^{2-})_2]^0$, which contains a tetravalent Si ion and two $(bpy^{2-})^{2-}$ dianions. It should not be described as $[Si^0(bpy^0)_2]^0$. For the heavier Ge, Sn, and Pb congeners the divalent state, characterized by a stereochemically active electron pair, becomes increasingly significant and dominates in 4-coordinate Sn and Pb species.

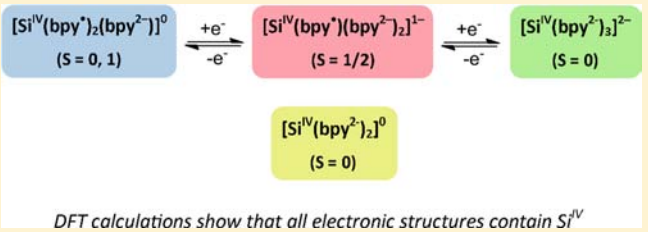

DFT calculations show that all electronic structures contain Si^{IV}

INTRODUCTION

In 1963, Herzog and Krebs reported the synthesis of a black, air sensitive microcrystalline material formulated as $[Si(bpy)_3]^0$ (bpy = 2,2′-bipyridine).[1] It was described as a Si^0 compound, which implies that the three bpy ligands are neutral, and reported to display a temperature-dependent magnetic moment that varies between 0.31 μ_B at 82 K and 1.29 μ_B at 410 K.[2] The latter was interpreted as deriving from an equilibrium between a Si^0 singlet ground state and a Si^0 triplet excited state, and although its use is wholly incorrect in such a scenario, the magnetic data was successfully fit with the Heisenberg−Dirac−van Vleck spin Hamiltonian ($\hat{H} = -2J \cdot S_1 \cdot S_2$; $S_1 = S_2 = 1/2$) using a J-coupling constant of -374 cm^{-1}. No further spectroscopic or theoretical investigations of this material have, to the best of our knowledge, been published since.

Interestingly, in 1979 the synthesis of a neutral black compound containing only *two* *N,N′*-coordinated bpy ligands, namely $[Si(bpy)_2]^0$, was described.[3] This compound was obtained as a crystalline solid, along with one equivalent of uncoordinated (bpy^0), upon attempts to sublime $[Si(bpy)_3]^0$ at 180 °C in vacuo.[4] It was found to be *diamagnetic* (S = 0) at ambient temperatures, and its structure was analyzed by X-ray crystallography (reasonably good quality data was obtained).[3] Once again, the authors described it as a zerovalent silicon compound, from which the presence of two neutral (bpy^0) ligands are inferred. However, this electronic structure assignment is questionable because the metrical parameters of the bpy ligands in the crystal structure of $[Si(bpy)_2]^0$ (see Table 3) imply a more reduced state.

In addition, in 1967 Herzog et al. reported that reduction of $[Si(bpy)_3]^0$ in tetrahydrofuran (THF) using $Na^+(bpy^{\bullet})^-$ affords a very air-sensitive black salt $Na[Si(bpy)_3]\cdot 7THF$, whose μ_{eff} at ambient temperature of 1.71 μ_B is indicative of an S = 1/2 ground state.[5] The corresponding lithium salt $Li[Si(bpy)_3]\cdot 3(bpy)$ was also prepared, but via an alternative synthetic route involving reaction of $SiCl_4$ with 5 equiv of $Li^+(bpy^{\bullet})^-$ in the presence of a slight excess of (bpy^0) (eq 1).

$$SiCl_4 + 5Li(bpy^{\bullet}) \xrightarrow[(bpy^0)]{THF} Li[Si(bpy)_3]\cdot 3(bpy) + 4LiCl \quad (1)$$

The same authors also described further reduction of the monoanion $[Si(bpy)_3]^-$ by one electron to yield the dianion $[Si(bpy)_3]^{2-}$ (eq 2). Black microcrystals of the latter were found to be diamagnetic at ambient temperature. Beyond measurement of their magnetic moments, the electronic structures of the three-membered electron transfer series $[Si(bpy)_3]^n$ (n = 0, 1−, 2−; Scheme 1) have yet to be investigated in any detail.

$$[Si(bpy)_3]^- + Li_{solid} \xrightarrow{THF} Li_2[Si(bpy)_3]\cdot 8THF \quad (2)$$

It should also be noted that the pale yellow or colorless compound $[Si(bpy)Cl_4]^0$ has been isolated from reaction of $SiCl_4$ with (bpy^0).[1,6] The crystal structure of this compound has yet to be reported, but those of the comparable species

Received: May 31, 2013
Published: August 9, 2013

   dx.doi.org/10.1021/ic401375a | *Inorg. Chem.* 2013, 52, 10067−10079

Scheme 1. Known Silicon bpy Compounds[1−3,6,22]

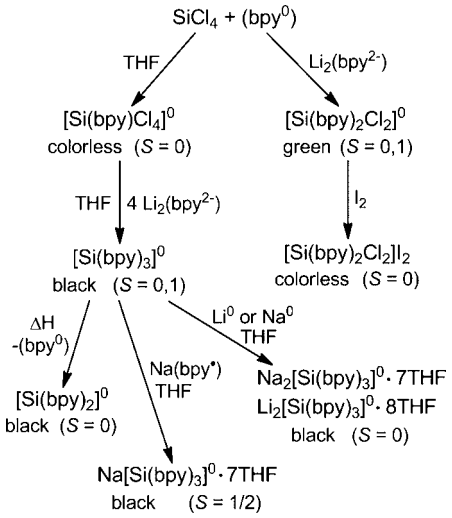

$[Si^{IV}(bpy^0)(N_3)_4]^0$ ($S = 0$)[7] and $[Si^{IV}(bpy^0)F_4]^0$ ($S = 0$)[8] are known, and are comprised of a $\{Si^{IV}(bpy^0)\}^{4+}$ moiety coordinated to four monoanions. Finally, a green microcrystalline product $[Si(bpy)_2Cl_2]^0$ was mentioned in reference 5, but little characterizational data was provided. However, its two electron oxidized form $[Si(bpy)_2Cl_2]^{2+}$ is well characterized, and its X-ray crystal structure is known.[27]

In a series of recent papers we[9] and others[10] have shown that on the basis of high-quality X-ray crystallography alone it is possible to experimentally determine the oxidation level of a bpy ligand in a given five-membered E(bpy) (E = transition metal ion) chelate ring, with it being either neutral (bpy^0), a $(bpy^{\bullet})^-$ π-radical anion, or a $(bpy^{2-})^{2-}$ dianion (see Scheme 2 and Table 1). In addition to a plethora of experimental techniques, broken symmetry (BS) density functional theory (DFT) calculations have proven to be invaluable in validating these conclusions and highly reliable in terms of accurately predicting the ground state electronic structures of such complexes.[9,10] As an extension of these studies, we have sought to obtain insight into the electronic structures of the long-overlooked silicon bpy compounds detailed above and summarized in Scheme 1, by performing a DFT study of these molecules, plus their germanium, tin, and lead congeners. The questions we seek to answer pertain to assignment of the physical oxidation states of the central group 14 element (+IV, +II, or 0) and the supporting bpy ligands (Scheme 2), and whether the principles that have been established for "low-valent" transition metal bpy complexes are equally applicable to p-block chemistry.

Scheme 2. Oxidation States of the bpy Ligand, Plus Averaged Crystallographically Determined Bond Distances[a]

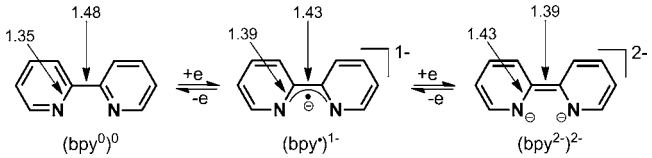

[a]Å, with error ∼ ±0.01 Å. Note, the intrachelate (C_{py}–C_{py} and C–N) bonds highlighted are the focus of all subsequent ligand structure discussions.

Table 1. Comparison of Average Experimental Bond Distances (± 0.01 Å) in Uncoordinated 2,2-bipyridine $(bpy)^0$ and Alkali Salts of the Corresponding Monoanion $(bpy^{\bullet})^-$ and Dianion $(bpy^{2-})^{2-}$[a]

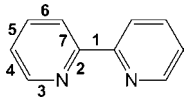

bond	(bpy^0)	$(bpy^{\bullet})^-$	$(bpy^{2-})^{2-}$
1	1.49	1.43	1.40−1.36
2	1.35	1.39	1.44
3	1.34	1.34	1.34
4	1.38	1.38	1.38
5	1.38	1.40	1.43
6	1.38	1.36	1.36
7	1.39	1.43	1.45

[a]Data taken from ref 4. A bond labeling scheme is provided with the table.

CALCULATIONS

All DFT calculations were performed using version 2.9 of the ORCA software package.[11] The geometries of all complexes were optimized, in redundant internal coordinates without imposing geometry constraints, and all subsequent single point calculations were performed at the B3LYP level of theory.[12] In all calculations, the def2-TZVP basis set was applied to all atoms.[13] For compounds incorporating Sn and Pb ions the zeroth-order regular approximation (ZORA) method was implemented.[14] In these calculations ZORA-TZVP replaces the TZVP basis sets.[14d] Auxiliary basis sets, used to expand the electron density in the calculations, were chosen to match the orbital basis sets.[15] The RIJCOSX and RIJONX approximations were used to accelerate the calculations.[16] The authenticity of each converged structure was confirmed by the absence of imaginary vibrational frequencies.

The self-consistent field calculations were tightly converged (1×10^{-8} E_h in energy, 1×10^{-7} E_h in the density charge, and 1×10^{-7} in the maximum element of the DIIS[17] error vector). In all cases, the geometries were considered converged after the energy change was less than 1×10^{-6} E_h, the gradient norm and maximum gradient element were smaller than 3×10^{-5} and 1×10^{-4} E_h $Bohr^{-1}$, respectively, and the root mean displacements of all atoms were smaller than 6×10^{-4} and 1×10^{-3} Bohr, respectively.

The B3LYP functional was selected after performing "test" calculations using a range of functionals (i.e., BP86, BLYP, B3LYP, and BHLYP) that incorporate varying amounts of Hartree−Fock exchange. Their performance was assessed based upon closeness of agreement between calculated and experimental results. More specifically, the structural parameters in geometry optimization structures of $[Si(bpy)_2]^0$, $[Pb(bpy)_2]^{2+}$, and $[M(bpy)Cl_2]^0$ (M = Ge, Sn) were compared with previously reported X-ray crystal structures (see Tables S12, S13, S15, S16, S21, and S29 in the Supporting Information). In all cases, geometry optimization for all functionals converged to approximately the same structures (any exceptions are discussed below). There was a small but noticeable decrease in bond lengths, particularly those in the bpy unit, with increasing amounts of Hartree−Fock exchange, and the best agreement with experimental structures was in most cases obtained using the B3LYP and BHLYP functionals. Additionally, electron−electron exchange coupling constants, J,

dx.doi.org/10.1021/ic401375a | Inorg. Chem. 2013, 52, 10067−10079

were calculated for $[Si(bpy)_3]^0$ using the BS(1,1) methodology via the Yamaguchi method (see below). The J_{calcd} value obtained using the B3LYP functional was found to display the best agreement with experiment. Hence, given the relative insensitivity of calculated geometry to experiment, the B3LYP functional was judged to give the best approximation to experiment and used throughout.

Throughout this study, our computational results are described using the broken symmetry (BS) approach.[18] The following notation is used to describe the BS solutions, where the given system is divided into two fragments. The notation BS(m,n) refers to an open-shell BS state with m unpaired α-spin electrons localized on fragment 1 and n unpaired β-spin electrons localized on fragment 2. In this notation the standard high-spin, open-shell solution is written as BS(m+n,0). The BS(m,n) notation refers to the initial guess for the wave function. The variational process does, however, have the freedom to converge to a solution of the form BS($m-n$,0), in which the $n\beta$-spin electrons effectively pair up with $n < m$ α-spin electrons on the partner fragment. Such a solution is then a standard $M_s \cong (m - n)/2$ spin-unrestricted or spin-restricted Kohn–Sham solution. As explained elsewhere,[19] the nature of the solution is investigated from the corresponding orbital transformation (COT), with the corresponding orbital overlaps indicating whether the system should be described as a spin-coupled or a closed-shell solution. Orbitals and density plots were created using Chimera.[20]

RESULTS

1.1. Compounds $[M(bpy)F_4]^0$ (M = Si, Ge, Sn, Pb). Whereas the crystal structures of the diamagnetic neutral compounds $[M(bpy)F_4]^0$ (M = Si, Ge, Sn) have been reported,[8] the corresponding Pb compound is currently not known. The former three display slightly distorted octahedral MN_2F_4 polyhedra, in which the two bpy nitrogen donors are in the equatorial plane. Unsurprisingly, in all three cases the C_{py}–C_{py} and C–N distances of the N,N'-coordinated bpy ligands (Supporting Information, Table S1) are unequivocally those of a neutral (bpy^0) ligand, and the central Si, Ge, and Sn atoms have an oxidation state of +IV.

Other than a slight overestimation of the M–N and M–F bond distances (≤0.09 Å), which is typically seen for the B3LYP functional, the corresponding geometry optimized structures of $[M(bpy)F_4]^0$ (M = Si, Ge, Sn; S = 0) obtained from spin-restricted Kohn–Sham (RKS) DFT calculations display excellent agreement with experiment (Supporting Information, Table S1). Consistent with expectations, the qualitative frontier molecular orbital (FMO) diagrams of the Si, Ge, and Sn compounds (Figure 1 and Supporting Information, Figures S13 and S14, respectively) are effectively identical, with the highest occupied molecular orbital (HOMO) and lowest unoccupied molecular orbital (LUMO) in each case being a π- and π^*-orbital of the bpy ligand (≤1% M character), respectively.

A stable RKS solution was also obtained for the hypothetical molecule $[Pb(bpy)F_4]^0$ (S = 0). Its geometry optimized structure is isostructural with its Si, Ge, and Sn analogues, so displays a long C_{py}–C_{py} bond of 1.491 Å that is characteristic of a neutral (bpy^0) ligand. Correspondingly, its electronic structure is best described as $[Pb^{IV}(bpy^0)F_4]^0$ (Supporting Information, Figure S15) Additionally, the average calculated Pb–F distance of 2.045 Å is comparable to the terminal Pb–F bonds lengths of 1.967 Å in $Pb^{IV}F_4$.[21] (The latter has a sheet structure containing $Pb^{IV}F_6$ octahedra.)

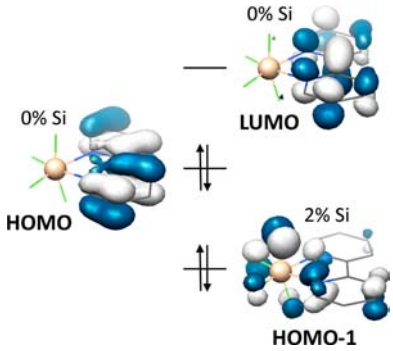

Figure 1. Qualitative FMO diagram for $[Si^{IV}(bpy^0)F_4]^0$ (S = 0).

1.2. Compounds *cis*-$[M(bpy)_2Cl_2]^n$ (M = Si, Ge, Sn, Pb; n = 2+ or 0). The diamagnetic complexes $[Si(bpy)_2Cl_2]X_2$ (X = Cl, I) have both been reported, but only the iodide salt has been characterized by X-ray crystallography.[22] This structure exhibits an octahedral SiN_4Cl_2 polyhedron, in which the two chlorine atoms are coordinated *cis* to one another and the metrical parameters of the two equivalent bpy ligands (Supporting Information, Table S2) correspond to a (bpy^0) oxidation state. As expected, its electronic structure is therefore $[Si^{IV}(bpy^0)_2Cl_2]^{2+}$. Performing a RKS geometry optimization provided a structure displaying excellent agreement with experiment, albeit with a ∼0.06 Å overestimation of the Si–N bond distances (Supporting Information, Table S2). Importantly, these calculations yielded two degenerate LUMOs, both of which are (bpy^0)-centered π^*-orbitals containing less than 2% Si character (Figure 2).

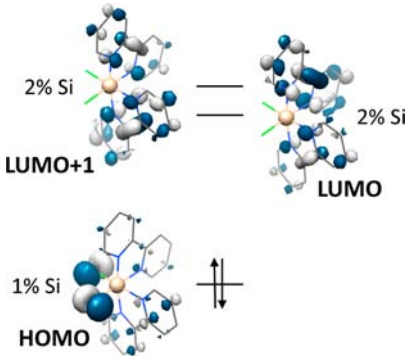

Figure 2. HOMO and two degenerate LUMOs of S = 0 $[Si^{IV}(bpy^0)_2Cl_2]^{2+}$.

Addition of two electrons to the aforementioned dication yields the neutral species $[Si(bpy)_2Cl_2]^0$. Calculations performed using the BS(1,1) formalism (S = 0) yielded a solution 5.5 and 0.5 kcal mol^{-1} lower in energy than the respective RKS (S = 0) and S = 1 (UKS) variants (Supporting Information, Table S3). Using the BS(1,1) geometry optimized structure, an antiferromagnetic coupling constant J_{calcd} of −84 cm^{-1} was calculated via the Yamaguchi approach (eq 3). (The meaning of the energies E_{HS} and E_{BS} and spin expectation values $\langle S^2 \rangle$ are described in ref 23).

$$J = -\frac{E_{HS} - E_{BS}}{\langle S^2 \rangle_{HS} - \langle S^2 \rangle_{BS}} \quad (3)$$

dx.doi.org/10.1021/ic401375a | Inorg. Chem. 2013, 52, 10067–10079

Hence, the neutral species possesses a BS(1,1) $S = 0$ ground state. In this geometry optimized structure, which is an octahedral *cis*-SiN_4Cl_2 polyhedron, the intrachelate $C_{py}-C_{py}$ and C−N bond lengths (1.421 and 1.392 Å, respectively) in the two identical bpy ligands clearly indicate (Scheme 2, Table 1) that they are $(bpy^{\bullet})^-$ π-radical anions and, by extension, the electronic structure of this molecule is best described as *cis*-$[Si^{IV}(bpy^{\bullet})_2Cl_2]^0$. Indeed, in its qualitative FMO diagram (Figure 3) two unpaired electrons of opposing spin reside in

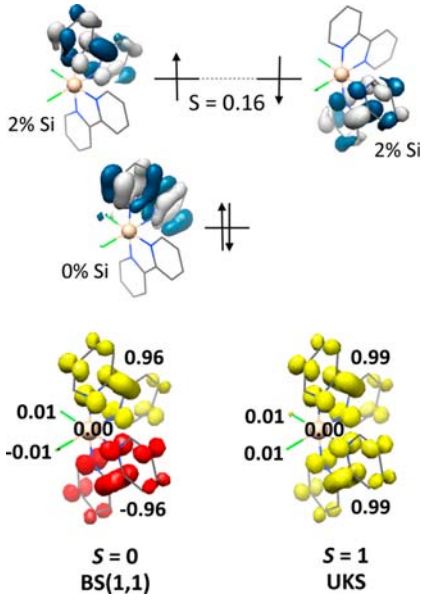

Figure 3. Qualitative FMO diagram for $S = 0$ *cis*-$[Si^{IV}(bpy^{\bullet})_2Cl_2]^0$ and Mulliken spin density plots, plus spin density populations, obtained from calculation of the $S = 0$ and $S = 1$ spin states using the BS(1,1) and UKS formalisms, respectively.

two degenerate singly occupied molecular orbitals (SOMOs), each of which are localized on a single bpy ligand (~2% Si character) and correspond to the two LUMOs in the dication $[Si^{IV}(bpy^0)_2Cl_2]^{2+}$. This is reflected in the Mulliken spin population analysis, which places 0.96 α-spins on one bpy ligand, 0.96 β-spins on the other, and 0.00 on the Si atom.

Calculations have also been performed for the corresponding germanium compounds *cis*-$[Ge(bpy)_2Cl_2]^n$ (n = 2+, 0). As expected, geometry optimization for the dication using the RKS ($S = 0$) formalism yielded a solution with structural parameters (Supporting Information, Table S5), in excellent agreement with formulation as $[Ge^{IV}(bpy^0)_2Cl_2]^{2+}$. Results for the corresponding neutral species $[Ge(bpy)_2Cl_2]^0$ mirror those of its Si analogue, with the BS(1,1) solution found to be 7 kcal mol^{-1} lower in energy than the RKS one. Additionally, an antiferromagnetic J_{calcd} of −26 cm^{-1} was calculated, leading to assignment of a BS(1,1) $S = 0$ ground state. Again the BS(1,1) optimized structure clearly contains $(bpy^{\bullet})^-$ ligands, as evidenced by the average $C_{py}-C_{py}$ bond length of 1.418 Å (Supporting Information, Table S5). Based upon the qualitative FMO and Mulliken spin density analysis (Supporting Information, Figures S19 and S2, respectively), it is apparent that the two weakly antiferromagnetically coupled unpaired electrons are localized in two ligand-centered π^*-orbitals (2% Ge), one on each bpy ligand. Therefore, the electronic structure of the neutral species is $[Ge^{IV}(bpy^{\bullet})_2Cl_2]^0$. Note that although both the dicationic and the neutral compounds of germanium-(IV) have yet to be reported, they are computationally stable and represent reasonable synthetic targets.

We have also calculated the dication $[Sn(bpy)_2Cl_2]^{2+}$ and its neutral analogue $[Sn(bpy)_2Cl_2]^0$, both of which are currently unknown. Geometry optimization of *cis*-$[Sn(bpy)_2Cl_2]^{2+}$ (S = 0), using the RKS formalism, reveals an octahedral *cis*-SnN_4Cl_2 geometry (Supporting Information, Table S3) with two neutral (bpy^0) ligands (the average $C_{py}-C_{py}$ bond length is 1.483 Å). Thus, as in the Si and Ge cases, the electronic structure is $[Sn^{IV}(bpy^0)_2Cl_2]^{2+}$ (Supporting Information, Figure S20).[22]

For the neutral species $[Sn(bpy)_2Cl_2]^0$, $S = 1$ and BS(1,1) $S = 0$ solutions can be found. The average $C_{py}-C_{py}$ distances of 1.425 Å in these solutions are indicative of the presence of two $(bpy^{\bullet})^-$ ligands (Supporting Information, Table S7), a notion reinforced by the corresponding spin density plots (Supporting Information, Figure S3), so the electronic structure description $[Sn^{IV}(bpy^{\bullet})_2Cl_2]^0$ is most appropriate for these neutral species. Interestingly, the RKS ($S = 0$) solution is 26 kcal mol^{-1} *lower* in energy than the two aforementioned solutions, and its geometry optimized structure exhibits bpy intraligand bond distances (Supporting Information, Table S7) that are typical of (bpy^0). Furthermore, it displays Sn−N distances of 2.8−3.2 Å, which are much longer than the 2.202 Å Sn−N bond lengths seen in the open shell solutions, and half of the *N*-donor atoms do not point toward the Sn ion. In effect, two neutral (bpy^0) molecules have dissociated and gaseous $Sn^{II}Cl_2$ has been generated (eq 4). This is presumably a result of the increasing stability of the +II oxidation state as the group is descended. Such an outcome could not be predicted from the qualitative FMO of $[Sn^{IV}(bpy^0)_2Cl_2]^{2+}$, in which the two degenerate LUMOs are bpy-centered π^*-orbitals (Supporting Information, Figure S20).

$$[Sn^{IV}(bpy^{\bullet})_2Cl_2]^0 \rightarrow Sn^{II}Cl_2 + 2(bpy^0) \quad (4)$$

Attempts to calculate the hypothetical, neutral molecule $[Pb(bpy)_2Cl_2]^0$ yielded a stable RKS ($S = 0$) solution 53 kcal mol^{-1} *lower* in energy than the corresponding $S = 1$ one. (Note, all BS(1,1) calculations converged to RKS solutions.) As was the case for the Sn analogue, the RKS optimized geometry (Supporting Information, Table S9) contains two (bpy^0) fragments and displays Pb−N distances (2.8−3.1 Å) that correspond to extremely weak interactions (Supporting Information, Figure S23). Thus, it appears that $Pb^{II}Cl_2$ and two dissociated (bpy^0) molecules represent the most stable state in the gas phase.

In contrast, the analogous dication $[Pb(bpy)_2Cl_2]^{2+}$ ($S = 0$) is a computationally stable species. The RKS geometry optimized structure is a slightly distorted octahedron with two neutral (bpy^0) ligands, and average Pb−N and Pb−Cl bond lengths of 2.384 and 2.441 Å, respectively (Supporting Information, Table S3). Its electronic structure can therefore be described as $[Pb^{IV}(bpy^0)_2Cl_2]^{2+}$. It should be noted that the LUMO calculated for the dication (Supporting Information, Figure S22) is, in contrast to its Si, Ge, and Sn analogues, *not* a bpy-centered π^*-orbital. Instead, it is localized on the $PbCl_2$ moiety (30% Pb character).

1.3. Compounds $[M(bpy)Cl_2]^0$ (M = Si, Ge, Sn, Pb). Calculations for the hypothetical neutral molecule $[Si(bpy)Cl_2]^0$ ($S = 0$), using the RKS formalism, yields an optimized structure with a tetrahedral geometry and Si−Cl bonds 2.06 Å long, which is a comparable length to those experimentally observed in $SiCl_4$ (2.01 Å).[24] Other than this, the most salient structural feature of this molecule is that the bpy fragment

dx.doi.org/10.1021/ic401375a | *Inorg. Chem.* 2013, 52, 10067−10079

Table 2. Selected Bond Lengths Taken from RKS Geometry Optimized Structures of the $S = 0$ Compounds $[M(bpy)Cl_2]^0$ (M = Si, Ge, Sn, Pb)[a]

		Ge		Sn		Pb		
bonds	Si	*cis*	*trans*	*cis*	*trans*	*cis*	*trans*	*trans* exp.[b]
M−N(1)	1.720	2.948	2.139	2.717	2.362	2.824	2.495	2.494
M−N(2)	1.722	2.333	2.141	2.540	2.361	2.654	2.494	2.520
N(1)−C(1)	1.438	1.336	1.343	1.335	1.343	1.336	1.342	1.33
N(2)−C(2)	1.442	1.349	1.343	1.348	1.342	1.346	1.341	1.36
C(1)−C(2)	1.373	1.487	1.473	1.487	1.482	1.491	1.487	1.50
M−Cl	2.064	2.290	2.525	2.449	2.628	2.544	2.707	2.776
M−Cl	2.058	2.312	2.516	2.512	2.629	2.608	2.708	2.945

[a]Atom labeling scheme provided in Chart1. [b]Values are taken from ref 27; $[Pb(bpy)Cl_2]$ is a polymer with a (4 + 2) distorted *pseudo*-octahedral coordination environment.

displays features characteristic of a $(bpy^{2-})^{2-}$ dianion (Table 2, Chart 1).[4c] More specifically, the $C_{py}-C_{py}$ and C−N

Chart 1. Intrachelate Atom Labeling Scheme

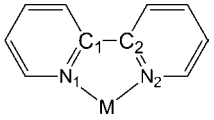

intrachelate bond distances of 1.373 and 1.440 Å correspond to C═C double and C−N single bonds, respectively. These structural parameters are consistent with the Si^{IV}-containing electronic structure $[Si^{IV}(bpy^{2-})Cl_2]^0$. The qualitative FMO diagram (Figure 4), in which the HOMO and LUMO are both bpy-centered π^*-orbitals (6% and 3% Si character, respectively), confirms this assignment.

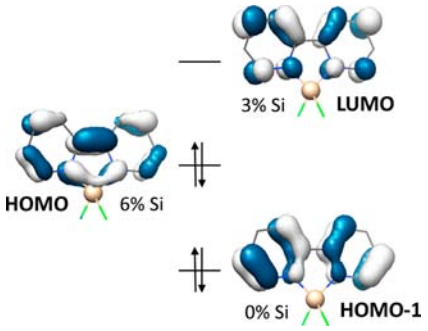

Figure 4. Qualitative FMO diagram for $[Si^{IV}(bpy^{2-})Cl_2]^0$ ($S = 0$).

The synthesis of $[Ge(bpy)Cl_2]^0$ and its characterization by X-ray crystallography have recently been reported.[25] The authors provided a detailed DFT study, at the B3LYP/cc-pvTZ level of theory, in which they found that the global energy minimum of the isolated molecule in the gas phase (two Cl ligands *cis* to one another) differs from the experimental geometry of the monomer in the solid state (two Cl ligands *trans* to one another). A geometry optimized structure corresponding to the latter could be located (both structures are depicted in Figure 5), but was found to be ∼10 kcal mol^{-1} higher in energy. Regardless, both isomers exhibit structural parameters indicative of a neutral (bpy^0) ligand and a stereochemically active electron pair, typical of divalent germanium, from which the electronic structure $[Ge^{II}(bpy^0)Cl_2]^0$ can be inferred.

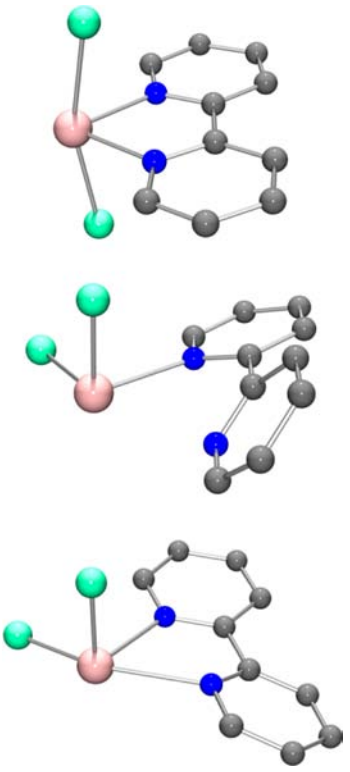

Figure 5. Geometry optimized structures of *trans*- and three coordinate *cis*-$[Ge^{II}(bpy^0)Cl_2]^0$ (top and middle, respectively) obtained using the B3LYP functional, and a four coordinate *cis*-$[Ge^{II}(bpy^0)Cl_2]^0$ (bottom) calculated using the BP86 functional.

Our own calculations using 4 different functionals (BP86, BLYP, B3LYP, BHLYP) reproduced these results, with the *trans* structure being ∼10 kcal mol^{-1} higher energy than the *cis* structure in all cases (Supporting Information, Table S11). It should be noted for the *cis* structure that using functionals containing increasing amounts of Hartree−Fock exchange caused elongation of one Ge−N bond to the extent that one ring of the *N,N′*-coordinated (bpy^0) ligand effectively dissociates (Supporting Information, Table S12), thereby lowering the coordination number from 4 to 3 (Figure 5). Reid et al. attributed the discrepancy between the calculated and experimental geometries to the nearest neighbor interactions observed in the solid state (effective coordination number = 4 + 2).[25] Modeling of these interactions by calculation of a tetramer yielded the observed solid state *trans*-structure as the global energy minimum. Regardless, no

dx.doi.org/10.1021/ic401375a | *Inorg. Chem.* 2013, 52, 10067−10079

evidence was found in any of the aforementioned calculations for the electronic structure $[Ge^{IV}(bpy^{2-})Cl_2]^0$ (see the qualitative FMO diagrams in Supporting Information, Figures S24 and S25). It is, therefore, clear that this germanium compound contains Ge^{II} and that the +IV oxidation state is not accessible.

Similarly, calculations for $[Sn(bpy)Cl_2]^0$ also converged to energy minima corresponding to the chloride ligands adopting both *cis*- and *trans*-positions relative to one another, with the former isomer once again being ~10 kcal mol^{-1} lower in energy than the latter for all four functionals mentioned above (Supporting Information, Table S14). In contrast to the Ge case, this is in agreement with the geometry observed in the crystal structure.[26] However, agreement between the calculated and observed Sn−N and Sn−Cl bond distances for the *cis*-isomer is very poor (Supporting Information, Table S15), presumably because our calculations do not incorporate the two additional weak chloride-to-tin interactions observed in the solid state (i.e., the effective coordination number is 6, not 4). On the other hand, it is clear both computationally and crystallographically that in this compound a neutral (bpy^0) is *N,N′*-coordinated to a central Sn^{II} ion, which displays a sterochemically active electron pair (Figure 6). In other words,

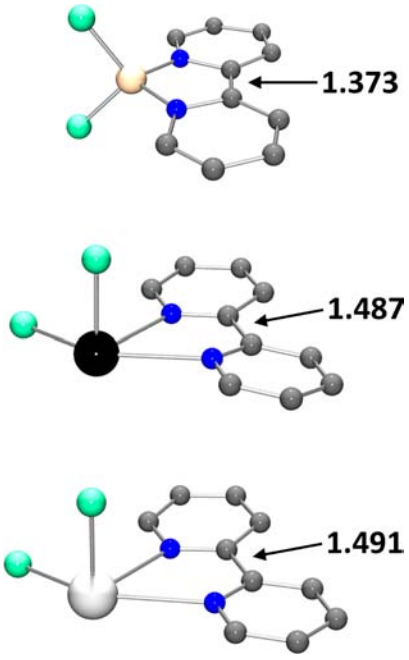

Figure 6. Geometry optimized structures of diamagnetic $[Si^{IV}(bpy^{2-})Cl_2]^0$ (top), $[Sn^{II}(bpy^0)Cl_2]^0$ (middle), and $[Pb^{II}(bpy^0)Cl_2]^0$ (bottom).

it has the electronic structure $[Sn^{II}(bpy^0)Cl_2]^0$. This is the case in both the *cis*- and *trans*-isomers and is reflected in their qualitative FMO diagrams (Supporting Information, Figures S26 and S27, respectively), in which the HOMOs are centered on the $SnCl_2$ and contain significant Sn character (44% and 28%, respectively), and the LUMOs are essentially bpy π^*-orbitals (≤1% Sn character).

Once again, RKS calculations for the neutral molecule $[Pb(bpy)Cl_2]^0$ (S = 0) affords both a *cis*- and a *trans*-isomer, with the former being 10.6 kcal mol^{-1} more stable than the latter. The structural parameters are consistent with a neutral (bpy^0) ligand (Table 3) and a stereochemically active inert pair of electrons (Figure 6), which lead to an oxidation state assignment of +II at the Pb center and the ground state electronic structure *cis*-$[Pb^{II}(bpy^0)Cl_2]^0$. Notably, in the *cis*-isomer both the calculated Pb−N and Pb−Cl bonds (Table 2) are elongated with an average length of 2.74 and 2.58 Å, respectively. The X-ray structure of $[Pb^{II}(bpy^0)Cl_2]^0$ has been published.[27] It is a polymer with bridging chloride ligands, a coordination number 6 at the Pb^{II} ion, and a long $C_{py}-C_{py}$ bond of 1.50(2) Å indicative of the presence of a neutral (bpy^0) ligand.

1.4. Series $[M(bpy)_2]^n$ (M = C, Si, Ge, Sn, Pb; n = 2+, 0). Calculation of geometry optimized structures for the neutral diamagnetic compound $[Si(bpy)_2]^0$, which has been characterized by X-ray crystallography,[3] were performed for the S = 2 (UKS), 1 (UKS), and 0 (RKS) states. (All BS(1,1) calculations converged to the RKS solution.) The single-point energy of the singlet state was found to be 24 and 53 kcal mol^{-1} lower in energy than the triplet and pentet states, respectively, so all subsequent discussions focus on the singlet state.

Other than the greater distortion away from tetrahedral symmetry in the experimental relative to the RKS calculated structure, which is evident in the respective angles between the two Si(bpy) planes of 72 and 84° (it is 90° in a regular tetrahedron), agreement between their structural parameters is excellent (Table 3). Most pertinently, the bpy units exhibit short $C_{py}-C_{py}$ and long C−N bonds (1.36 and 1.44 Å, respectively) characteristic of *N,N′*-coordinated $(bpy^{2-})^{2-}$ dianions (Table 1). This notion is confirmed by its qualitative FMO diagram (Figure 8) containing two degenerate bpy-centered HOMOs (7% Si character), which correspond to doubly occupied π^*-orbitals, and lead to formulation of its electronic structure as $[Si^{IV}(bpy^{2-})_2]^0$ (resonance structure **C**, Figure 7). It should be highlighted that there is no support, experimental or computational, for the $[Si^0(bpy^0)_2]^0$ electronic structure suggested by the original authors.[3]

The computational results for the hypothetical carbon containing compound $[C(bpy)_2]^0$ are very similar. More specifically, the RKS (S = 0) geometry optimized structure exhibits bond lengths indicative of the presence of two $(bpy^{2-})^{2-}$ dianions (Table 3), which implies that central carbon atom is tetravalent, and the dihedral angle between the two C(bpy) planes of 89° is consistent with the presence of a sp^3-hybridized central carbon atom. This equates to the electronic structure $[C^{IV}(bpy^{2-})_2]^0$ (S = 0), which is depicted pictorially by resonance structure **B** (Figure 7). Application of the oxidation formalism to carbon compounds may seem somewhat alien because of the high levels of covalency in C−C and C−H bonds, but the minimal contribution of the central carbon atom to the two bpy-centered HOMOs of this compound (Supporting Information, Figure S30) combined with the large electronegativity between C and N render such an electronic description reasonable. Though $[C(bpy)_2]^0$ has not been reported, other crystallographically characterized species containing a similar tetrahedral N_4C central moiety are known.[28] For example, $[C(N(CH_3)_2)_4]^0$ (tetrakis(dimethylamido)carbon), which has an average C−N bond length of 1.473 Å.[28b] The comparable Si compound $[Si^{IV}(NHCH_3)_4]^0$ (tetrakis(methylamido)silicon) has also been structurally characterized, and exhibits an average Si−N bond length is 1.720 Å.[29] These C−N and Si−N bond distances are in close agreement with the average values of 1.462 and 1.736 Å calculated for $[C(bpy)_2]^0$ and $[Si(bpy)_2]^0$, all of which are typical of single bonds.

dx.doi.org/10.1021/ic401375a | *Inorg. Chem.* 2013, 52, 10067−10079

Table 3. Selected Experimental[3] and Calculated Bond Distances (Å) in $[Si(bpy)_2]^{2+/0}$ and $[C(bpy)_2]^{2+/0a}$

bonds		$[Si(bpy)_2]^0$		$[Si(bpy)_2]^{2+}$	$[C(bpy)_2]^0$	$[C(bpy)_2]^{2+}$
		exp.	calcd.	calcd.	calcd.	calcd.
bpy(1)	M−N(1)	1.728(9)	1.745	1.747	1.462	1.466
	M−N(2)	1.711(9)	1.745	1.747	1.462	1.466
	N(1)−C(1)	1,44(1)	1.441	1.404	1.426	1.393
	N(2)−C(2)	1.44(1)	1.440	1.404	1.426	1.393
	C(1)−C(2)	1.35(1)	1.389	1.422	1.364	1.408
bpy(2)	M−N(1)	1.73(1)	1.745	1.747	1.462	1.466
	M−N(2)	1.71(1)	1.745	1.747	1.462	1.466
	N(1)−C(1)	1.44(1)	1.440	1.403	1.426	1.392
	N(2)−C(2)	1.43(1)	1.440	1.403	1.426	1.392
	C(1)−C(2)	1.34(1)	1.389	1.421	1.364	1.408

[a]Atom labeling scheme provided in Chart1.

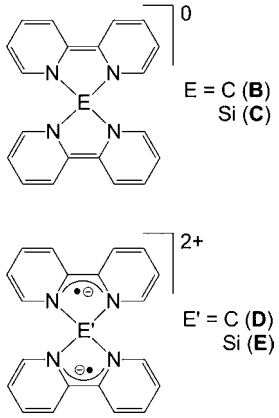

Figure 7. Dominant resonance structures for $[C^{IV}(bpy^{2-})_2]^0$ (**B**), $[Si^{IV}(bpy^{2-})_2]^0$ (**C**), $[C^{IV}(bpy^{\bullet})_2]^{2+}$ (**D**), and $[Si^{IV}(bpy^{\bullet})_2]^{2+}$ (**E**).

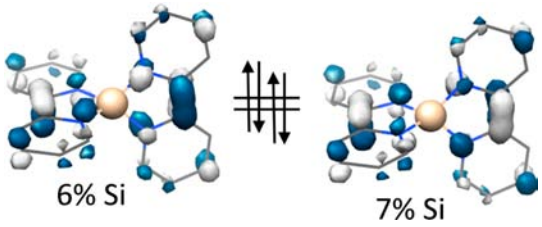

Figure 8. The two degenerate HOMOs of $[Si^{IV}(bpy^{2-})_2]^0$ (S = 0).

Oxidation of $[Si(bpy)_2]^0$ in silico affords the dication $[Si(bpy)_2]^{2+}$. The S = 0 RKS solution was found to be ∼4.7 kcal mol^{-1} higher in energy than those from the S = 1 and S = 0 BS(1,1) calculations. The latter two states are virtually isoenergetic, with a vanishingly small J_{calcd} of +3.7 cm^{-1} being obtained. While the average calculated Si−N bond length in the neutral and dicationic species (1.747 Å in both cases) are unperturbed by oxidation of the former to the latter, the effect upon the structural parameters of the bpy units is much greater (Table 3). For example, the average C_{py}−C_{py} bond length increases from 1.389 Å in the neutral compound to 1.422 Å in the dication and, conversely, the average calculated intrachelate C−N bond length decreases from 1.440 to 1.404 Å. The calculated bond lengths in the bpy moieties in the neutral species are typical of $(bpy^{2-})^{2-}$, but those in the dication closely resemble those of $(bpy^{\bullet})^-$ π-radical anions. Thus, the dication is most correctly defined as $[Si^{IV}(bpy^{\bullet})_2]^{2+}$ (resonance structure **E**) and is likely to have an S = 1 ground state and a singlet diradical excited state. This model is corroborated by the qualitative FMO scheme shown in Figure 9, containing two degenerate bpy-centered SOMOs (≤2% Si character), and the

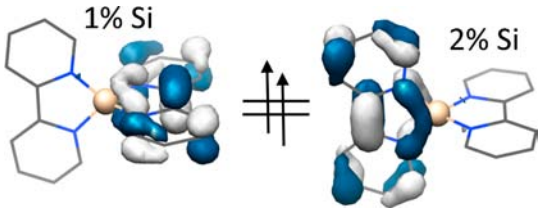

Figure 9. The two degenerate SOMOs of S = 1 $[Si^{IV}(bpy^{\bullet})_2]^{2+}$.

Mulliken spin density analysis, which places 0.91 unpaired spins on each $(bpy^{\bullet})^-$ ligand and only 0.18 at the central Si^{IV} ion.

Calculations for $[C(bpy)_2]^{2+}$ yield an analogous outcome, with the S = 0 RKS solution being >5 kcal mol^{-1} higher in energy than the S = 1 and S = 0 BS(1,1) states. However, in this case, the latter two solutions are not fully isoenergetic, and a significant ferromagnetic J_{calcd} = +71 cm^{-1} was found. As observed for its Si congener, in the S = 1 ground state the average C_{py}−C_{py} and intrachelate C−N bond lengths (1.408 and 1.392 Å, respectively) are typical of $(bpy^{\bullet})^-$; the average C−N distances of the CN_4 polyhedron (1.466 Å) are near identical to that of $[C^{IV}(bpy^{2-})_2]^0$; its qualitative FMO diagram (Supporting Information, Figure S29) contains two bpy-centered SOMOs (≤4% central C atom character); and the Mulliken spin density analysis places minimal spin density on the central C atom (Supporting Information, Figure S4). Hence, the electronic structure of the dication is best described as being $[C^{IV}(bpy^{\bullet})_2]^{2+}$ (resonance structure **D**, Figure 7), with an S = 1 ground state and a BS(1,1) excited state. The orthogonality of the bpy ligands in $[C^{IV}(bpy^{\bullet})_2]^{2+}$ and $[Si^{IV}(bpy^{\bullet})_2]^{2+}$ prohibit antiferromagnetic coupling of the ligand radicals, so result in positive J-values, and the larger interaction between the unpaired spins in the former is simply a consequence of greater orbital overlap with the central atom that mediates it.

It is now interesting to explore the molecular and electronic structures of the corresponding Ge, Sn, and Pb analogues $[M(bpy)_2]^{2+/0}$ (M = Ge, Sn, Pb), for which the divalent oxidation state of the central atom is expected to become increasingly prominent. Indeed, the $[Pb(bpy)_2]^{2+}$ dications in the X-ray crystal structures of the diamagnetic (S = 0) compounds $[Pb(bpy)_2](PF_6)_2$[30a] and $[Pb(bpy)_2][B_{12}H_{12}]$[30b] have been found to display a stereochemically active electron pair indicative of a +II oxidation state. Geometry optimization

dx.doi.org/10.1021/ic401375a | Inorg. Chem. 2013, 52, 10067−10079

of the dication $[Pb(bpy)_2]^{2+}$ using the RKS formalism (no BS solution could be found and the $S = 1$ state is 65 kcal mol^{-1} higher in energy) converged to a very similar structure (Figure 10), in which two neutral (bpy^0) ligands (Table 4) are *N,N′*-

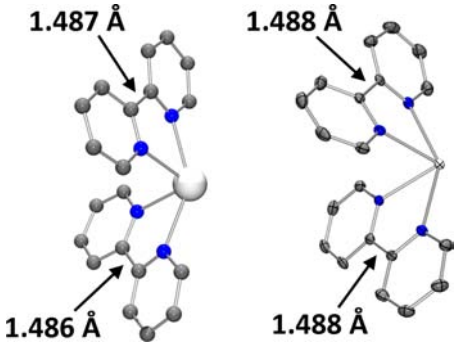

Figure 10. Calculated (left) and experimental[30a] (right) structures of $[Pb^{II}(bpy^0)_2]^{2+}$ ($S = 0$).

coordinated to a central Pb^{II} ion exhibiting a streochemically active lone pair (Supporting Information, Figure S36). Thus, both experimentally and computationally, its electronic structure is $[Pb^{II}(bpy^0)_2]^{2+}$.

For the neutral species $[Pb(bpy)_2]^0$, calculations for the $S = 1$ (UKS) and 0 (RKS and BS(1,1)) states were performed. The RKS solution was found to be ~2 kcal mol^{-1} higher in energy than the $S = 1$ and BS(1,1) states, and to exhibit a significantly different geometry optimized structure. In the RKS case, one of the bpy ligands completely dissociates and has bond lengths typical of (bpy^0), whereas the other remains *N,N′*-coordinated and is a $(bpy^{2-})^{2-}$ dianion (Table 4). In contrast, the $S = 1$ and BS(1,1) geometry optimized structures retain the general structure of $[Pb^{II}(bpy^0)_2]^{2+}$, possessing a sterochemically active electron pair, but the average $C_{py}-C_{py}$ bond length of 1.430 Å is indicative of two $(bpy^{\bullet})^-$ radical anions being present (Table 4 and Supporting Information, Table S31). The Mulliken spin density plots and population analyses (Supporting Information, Figure S6) confirm that one unpaired electron resides in each of the bpy-centered SOMOs, and that there is no significant spin density at Pb. Furthermore, a ferromagnetic J_{calcd} of +38 cm^{-1} was calculated, which suggests that the neutral molecule has a $S = 1$ $[Pb^{II}(bpy^{\bullet})_2]^0$ ground state. Given that the RKS solution is very close in energy, experimentally $\{[Pb^{II}(bpy^{2-})]^0 + (bpy^0)\}$ is an equally feasible outcome.

Calculations for $[Sn(bpy)_2]^{2+/0}$ yielded very similar results to those for $[Pb(bpy)_2]^{2+/0}$. The RKS optimized geometry for the $S = 0$ dication exhibits a stereochemically active electron pair, an average $C_{py}-C_{py}$ distance of 1.482 Å (Supporting Information, Table S27), which is typical of two neutral (bpy^0) ligands, and its qualitative FMO contains a HOMO with 48% Sn character and two near-degenerate bpy-centered LUMOs (Supporting Information, Figure S34). In other words, its electronic structure can be described as $[Sn^{II}(bpy^0)_2]^{2+}$. Additionally, for the neutral complex $[Sn(bpy)_2]^0$ the lowest energy solutions were the near degenerate $S = 1$ and BS(1,1) states (J_{calcd} = +31 cm^{-1}), with the RKS equivalent ~3 kcal mol^{-1} higher in energy. The structural and electronic descriptions of these various states are effectively identical to those described above for $[Pb(bpy)_2]^0$. Therefore, although both of the structures $[Sn^{II}(bpy^{\bullet})_2]^0$ and $\{[Sn^{II}(bpy^{2-})]^0 + bpy^0\}$ are considered to be feasible, the central Sn atom has a +II oxidation state in both scenarios.

Interestingly, unlike its Si, Sn, or Pb analogues, the structure obtained from geometry optimization of $[Ge(bpy)_2]^{2+/0}$ was found to be highly dependent upon the starting point. When starting geometries displaying distortions associated with a stereochemically active lone pair were used similarly distorted Ge^{II} optimized structures were obtained, but in several instances calculation using a tetrahedral starting point converged to a tetrahedral Ge^{IV} optimized geometry (Supporting Information, Table S25). However, for all states calculated the geometry optimized structures with a stereochemically active electron pair were found to be significantly lower in energy (Supporting Information, Table S24), and only these Ge^{II} solutions are discussed hereafter. Beyond this unique facet, the results of the calculations summarized in Figure 11 and Table 4 are quite similar to those found for the corresponding Sn and Pb compounds. For example, the ground state of the dication contains two neutral (bpy^0) ligands and a Ge^{II} center (its HOMO has 48% Ge character, Supporting Information, Figure S31), so its electronic structure is best described as $[Ge^{II}(bpy^0)_2]^{2+}$ ($S = 0$).

Calculations of BS(1,1) and $S = 1$ (UKS) states for the neutral species $[Ge(bpy)_2]^0$ yield a very similar distorted GeN_4

Table 4. Selected Calculated Bond Distances (Å) and Angles (deg) for the $S = 0$ Compounds $[M(bpy)_2]^n$ (M = Ge, Sn, Pb; n = 2+, 0)[a]

		$[M(bpy)_2]^{2+b}$				$\{M(bpy) + (bpy^0)\}^b$			$[M(bpy)_2]^{0c}$		
bonds		Ge	Sn	Pb	Pb exp.[d]	Ge	Sn	Pb	Ge	Sn	Pb
bpy(1)	M–N(1)	2.115	2.336	2.540	2.553	1.922	2.150	2.203	2.082	2.279	2.496
	M–N(2)	2.230	2.431	2.452	2.518	1.922	2.162	2.316	2.231	2.378	2.391
	N(1)–C(1)	1.359	1.355	1.347	1.339	1.398	1.393	1.388	1.395	1.389	1.377
	N(2)–C(2)	1.347	1.347	1.352	1.328	1.400	1.392	1.384	1.373	1.375	1.386
	C(1)–C(2)	1.476	1.482	1.486	1.488	1.399	1.411	1.420	1.421	1.426	1.429
bpy(2)	M–N(1′)	2.126	2.337	2.449	2.518				2.086	2.281	2.390
	M–N(2′)	2.306	2.434	2.538	2.532				2.252	2.382	2.500
	N(1′)–C(1′)	1.358	1.355	1.353	1.328	1.337	1.338	1.339	1.394	1.389	1.386
	N(2′)–C(2′)	1.346	1.347	1.347	1.339	1.338	1.338	1.339	1.371	1.375	1.378
	C(1′)–C(2′)	1.475	1.482	1.487	1.488	1.491	1.491	1.490	1.421	1.425	1.429
N(1)–M–N(1′)		161.5	150.3	146.1	139.8				159.5	150.0	146.9
N(2)–M–N(2′)		92.2	90.5	91.6	72.8				93.5	90.5	91.0

[a]Atom labeling scheme provided in Chart1. [b]RKS calculation. [c]BS(1,1) calculation. [d]Taken from ref 30.

dx.doi.org/10.1021/ic401375a | *Inorg. Chem.* 2013, 52, 10067−10079

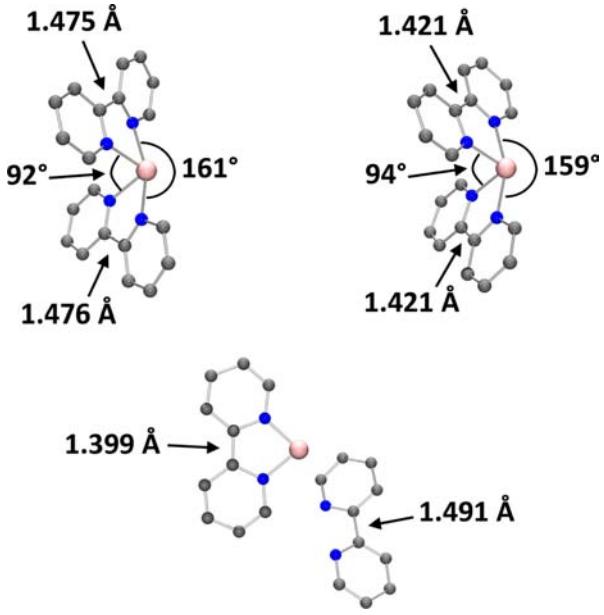

Figure 11. Geometry optimized structures of $[Ge^{II}(bpy^0)_2]^{2+}$ (top left), $[Ge^{II}(bpy^{\bullet})_2]^0$ (top right), and $\{[Ge^{II}(bpy^{2-})]^0 + (bpy^0)\}$ (bottom) obtained from RKS (S = 0), UKS (S = 1), and RKS (S = 0) calculations, respectively.

polyhedron (Figure 11), and an electronic structure $[Ge^{II}(bpy^{\bullet})_2]^0$ containing a Ge^{II} ion and two $(bpy^{\bullet})^-$ radicals is identified (Supporting Information, Figure S7). In contrast to its Sn and Pb analogues, the RKS solution (S = 0) is ∼6 kcal mol^{-1} *lower* in energy than the open-shell solutions, so represents the global energy minimum, but it retains a similar structure composed of one dissociated neutral (bpy^0), and a $[Ge^{II}(bpy^{2-})]^0$ fragment composed of a Ge^{II} ion *N,N′*-coordinated by a single $(bpy^{2-})^{2-}$dianion (Supporting Information, Figure S32).

1.5. Series $[M(bpy)_3]^n$ (M = Si, Ge, Sn, Pb; *n* = 1+, 0, 1−, 2−). Calculations for the dianion $[Si(bpy)_3]^{2-}$ yielded a closed-shell ground state (the S = 1 state was 18.5 kcal mol^{-1} higher in energy and no BS could be found) whose structure contains three equivalent bpy ligands *N,N′*-coordinated in a nearly regular octahedral fashion (it exhibits a twist angle Θ of ∼53°, and that of a regular octahedron is 60°). The short average calculated $C_{py}-C_{py}$ bond length of 1.371 Å and the long average intrachelate C−N bond distance of 1.428 Å (Table 5) are very similar to those observed in structures of alkali metal salts of $(bpy^{2-})^2$ dianions[4c] (Scheme 2, Table 1). Congruently, its qualitative FMO diagram (Supporting Information, Figure S42) contains three doubly occupied bpy-centered HOMOs (≤3% Si character), which inexorably leads to the electronic structure assignment $[Si^{IV}(bpy^{2-})_3]^{2-}$.

Geometry optimization for the monoanion $[Si(bpy)_3]^-$ (S = 1/2) using the UKS formalism (no BS solutions were found) yielded a similar octahedral structure (Θ = 54°) containing three nearly equivalent bpy-ligands, but with a slightly longer average $C_{py}-C_{py}$ bond length of 1.384 Å and a slightly shorter average C−N bond of 1.413 Å (Supporting Information, Table S37). These bond length changes indicate that one electron oxidation of the dianion to the monoanion is a ligand-centered process, which implies that the ligand oxidation level in the latter is $\{(bpy)_3\}^{5-}$. Accordingly, a Mulliken spin population analysis places 0.46 spins on one bpy ligand, 0.28 and 0.27 on each of the other two, and only 0.01 on the central Si^{IV} ion (Supporting Information, Figure S9); and the qualitative FMO diagram (Supporting Information, Figure S41) contains two degenerate bpy-centered HOMOs (3% Si character) and one bpy-centered SOMO (1% Si character). Thus, the electronic structure of the monoanion is most correctly described as $[Si^{IV}(bpy^{2-})_2(bpy^{\bullet})]^-$. Note, our calculations yield a structure in which the unpaired electron is delocalized over the three bpy ligands, but delocalization of charge is a known bias of DFT,[9] so a localized electronic structure with the unpaired electron on a single bpy ligand cannot be excluded. Indeed, performing the same calculation with the inclusion of the conductor-like screening model (COSMO) for water yielded a structure in which the single unpaired electron is almost fully localized on a single bpy ligand (Table 5 and Supporting Information, Figure S9).

Table 5. Selected Bond Distances (Å) from Geometry Optimized Structures of $[Si(bpy_3)]^n$ (n = 1+, 0, 1−, 2−)[a]

		n, S, method			
bond		1+, 1/2, BS(2,1)	0, 0, BS(1,1)	1−, 1/2, UKS[b]	2−, 0, RKS
bpy(1)	Si−Ni	1.907	1.872	1.884	1.907
	Si−N(2)	1.913	1.878	1.880	1.917
	N(1)−C(1)	1.388	1.410	1.427	1.428
	N(2)−C(2)	1.388	1.411	1.423	1.428
	C(1)−C(2)	1.415	1.390	1.376	1.371
bpy(2)	Si−N(1)	1.912	1.930	1.879	1.916
	Si−N(2)	1.908	1.930	1.886	1.907
	N(1)−C(1)	1.387	1.389	1.423	1.428
	N(2)−C(2)	1.388	1.389	1.427	1.428
	C(1)−C(2)	1.414	1.410	1.376	1.370
bpy(3)	Si−N(1)	1.913	1.912	1.961	1.918
	Si−N(2)	1.913	1.903	1.960	1.919
	N(1)−C(1)	1.387	1.400	1.390	1.427
	N(2)−C(2)	1.387	1.397	1.390	1.427
	C(1)−C(2)	1.413	1.400	1.407	1.371
average Si−N		1.911	1.904	1.908	1.914
average C(1)−C(2)		1.414	1.400	1.386	1.371

[a]Atom labeling scheme provided in Chart 1. [b]Calculation performed including the conductor-like screening model (COSMO)[31] for water.

dx.doi.org/10.1021/ic401375a | *Inorg. Chem.* 2013, 52, 10067−10079

Calculations were performed for the S = 1 (UKS) and 0 (RKS and BS(1,1)) states of the neutral species $[Si(bpy)_3]^0$. The BS(1,1) solution was found to be 2 kcal mol^{-1} lower in energy than the RKS one and 1.5 kcal mol^{-1} lower in energy than the S = 1 state. Thus, the electronic structure of the neutral species may be described as a singlet diradical, and using the Yamaguchi method (eq 3) a coupling constant J_{calcd} of −490 cm^{-1} was obtained, which is in good agreement with the experimental value of −374 cm^{-1}.[2] Based upon the calculated average C_{py}−C_{py} bond length of 1.400 Å, a collective bpy oxidation level of $\{(bpy)_3\}^{4-}$ can be deduced, which leads to the electronic structure assignment $[Si^{IV}(bpy^{\bullet})_2(bpy^{2-})]^0$ (S = 0). The qualitative FMO and the spin density plots shown in Figure 12 corroborate this assignment, but suggest that the

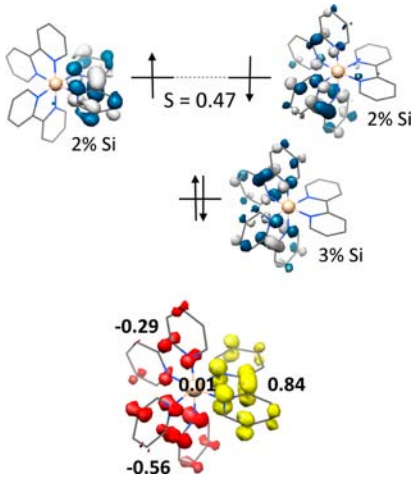

Figure 12. Qualitative FMO diagram and Mulliken spin density plot, plus spin density populations, for S = 0 $[Si^{IV}(bpy^{\bullet})_2(bpy^{2-})]^0$.

excess electron on the $(bpy^{2-})^{2-}$ is partly delocalized over one of the $(bpy^{\bullet})^-$ ligands. As a further point of interest, a fully localized structure *is* obtained when the geometry optimization is performed using the BHLYP functional (Supporting Information, Figures S8 and S40), which contains a larger amount of Hartree−Fock exchange. Using this functional, the BS(1,1) solution was found to be 14 kcal mol^{-1} lower in energy than the RKS one (Supporting Information, Table S32). However, the J_{calcd} value of −139 cm^{-1} obtained is in poorer agreement with experiment than that from the corresponding B3LYP calculation.

In the case of the monocation $[Si(bpy)_3]^+$ calculation of the S = 1/2 state converges to a BS(2,1) solution that is ∼1 kcal mol^{-1} lower in energy than the S = 3/2 excited state. A single-point calculation of the corresponding Yamaguchi exchange coupling constant, using the BS(2,1) optimized structure, yielded a J_{calcd} value of −179 cm^{-1}. The aforementioned optimized structure is again octahedral (Θ = 54°), and contains three fully equivalent bpy ligands whose C_{py}−C_{py} bond distances are typical of $(bpy^{\bullet})^-$ anions (Table 5). This picture is supported by its qualitative FMO diagram (Figure 13), which contains three bpy-centered SOMOs (≤3% Si character), and Mulliken spin density population analyses for the S = 1/2 ground and 3/2 excited states, both of which place approximately one full unpaired spin on each ligand and <0.01 on the Si atom. In other words, the monocation contains three π-radical monoanions $(bpy^{\bullet})^-$ and a central Si^{IV} ion, so has the electronic structure $[Si^{IV}(bpy^{\bullet})_3]^+$ (S = 1/2).

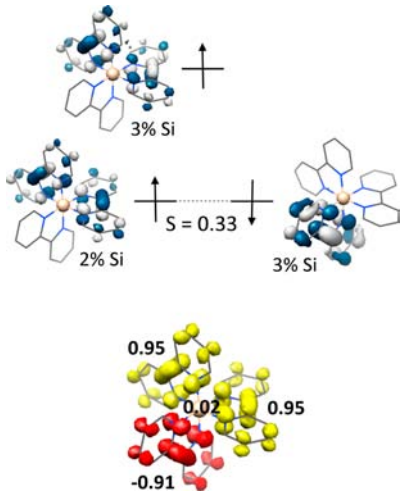

Figure 13. Qualitative FMO diagram and Mulliken spin density plot, plus spin density populations, for S = 1/2 $[Si^{IV}(bpy^{\bullet})_3]^+$.

We have also performed calculations for the theoretical neutral compounds $[M(bpy)_3]^0$ (M = Ge, Sn, Pb) using the same protocol. In the case of $[Ge(bpy)_3]^0$ we found that the BS(1,1) solution is 2.9 and 3.5 kcal mol^{-1} lower in energy than those from the S = 1 and RKS calculations, respectively. Similar observations were made for $[Sn(bpy)_3]^0$, with the BS(1,1) solution being 0.1 and 5.2 kcal mol^{-1} lower in energy than the S = 1 and RKS solutions. From single-point calculations antiferromagnetic exchange coupling constants J_{calcd} of −216 and −54 cm^{-1} were obtained for the Ge and Sn compounds, respectively. The progressive decrease in the magnitude of the antiferromagnetic J_{calcd} upon moving down the group from Si to Ge to Sn is presumably a consequence of the accompanying decrease in orbital overlap with the central group 14 atom, which mediates the interaction between the unpaired spins of the two $(bpy^{\bullet})^-$ ligands. Overall, the molecular (Table 6) and electronic (Supporting Information, Figures S43 and S44) structures of the Ge and Sn compounds are the same as that determined for their Si counterpart. More specifically, they

Table 6. Selected Bond Lengths (Å) Taken from BS(1,1) Geometry Optimized Structures of the S = 0 Compounds $[M(bpy)_3]^0$ (M = Ge, Sn, Pb)[a]

bonds		Ge	Sn	Pb
bpy(1)	M−N(1)	1.960	2.159	2.416
	M−N(2)	1.967	2.154	2.547
	N(1)−C(1)	1.411	1.405	1.389
	N(2)−C(2)	1.413	1.405	1.376
	C(1)−C(2)	1.390	1.403	1.430
bpy(2)	M−N(1)	2.045	2.212	3.338
	M−N(2)	2.048	2.210	3.588
	N(1)−C(1)	1.384	1.383	1.339
	N(2)−C(2)	1.385	1.383	1.339
	C(1)−C(2)	1.417	1.425	1.491
bpy(3)	M−N(1)	2.014	2.152	2.500
	M−N(2)	2.006	2.155	2.437
	N(1)−C(1)	1.400	1.406	1.380
	N(2)−C(2)	1.395	1.406	1.384
	C(1)−C(2)	1.404	1.402	1.430

[a]Atom labeling scheme provided in Chart 1.

dx.doi.org/10.1021/ic401375a | *Inorg. Chem.* 2013, 52, 10067−10079

possess the singlet (S = 0) diradical ground states $[Ge^{IV}(bpy^{\bullet})_2(bpy^{2-})]^0$ and $[Sn^{IV}(bpy^{\bullet})_2(bpy^{2-})]^0$.

Calculations for $[Pb(bpy)_3]^0$ revealed that the RKS solution is ~3.5 kcal mol^{-1} higher in energy than those for the BS(1,1) and S = 1 states. In contrast to the previously detailed $[M(bpy)_3]^0$ compounds, a ferromagnetic coupling constant J_{calcd} of +26 cm^{-1} was obtained, which suggest that the triplet state is the most stable electronic configuration. Additionally, subsequent to geometry optimization none of the aforementioned solutions retained the octahedral $[Pb(bpy)_3]^0$ starting geometry. Instead, in the open-shell structures one (bpy^0) ligand has dissociated (eq 5), whereas in the RKS solution two (bpy^0) ligands have dissociated (Supporting Information, Table S45). This presumably reflects the greater stability of the +II, relative to the +IV, oxidation state, which structurally manifests as a stereochemically active electron pair. The other notable feature of the S = 1 geometry optimized structure is that the average $C_{py}-C_{py}$ bond length of 1.430 Å (Table 6) is typical of $(bpy^{\bullet})^-$ π-radical anions. From these facts, plus the corresponding FMO diagram and spin density plot (Supporting Information, Figures S12 and S45), a $\{[Pb^{II}(bpy^{\bullet})_2]^0 + (bpy^0)\}$ (S = 1) ground state electronic structure can be inferred. However, given the close energetic proximity of the RKS solution, $\{[Pb^{II}(bpy^{2-})]^0 + 2\ (bpy^0)\}$ (S = 0) cannot be completely ruled out.

$$[Pb(bpy)_3]^0 \rightarrow [Pb^{II}(bpy^{\bullet})_2]^0 + (bpy^0) \quad (5)$$

DISCUSSION

As detailed above, the three lightest members of the series $[M^{IV}(bpy^0)F_4]^0$ (S = 0; M = Si, Ge, Sn, Pb) are known and have been crystallographically characterized, but $[Pb^{IV}(bpy^0)F_4]^0$ (S = 0) is at present only hypothetical. The agreement between the three experimental structures and the corresponding DFT calculated structures is excellent (Supporting Information, Table S1). In each case an octahedral geometry containing four fluoride anions, a neutral *N,N′*-coordinated bpy ligand and a central tetravalent ion are identified. Given that molecular $Si^{IV}F_4$ and $Ge^{IV}F_4$ (tetrahedral geometry), and polymeric $Sn^{IV}F_4$ and $Pb^{IV}F_4$ (sheet structures composed of octahedral SnF_6/PbF_6 polyhedra, in which the four equatorial fluorides are μ_2-bridging and two axial fluorides are terminally bound[21]) exist, the corresponding $[Pb^{IV}(bpy)F_4]^0$ species represents a feasible synthetic target. It should be noted that the $C_{py}-C_{py}$ and intrachelate C−N bond distances of the *N,N′*-coordinated planar bpy ligand in these compounds are near identical (Supporting Information, Table S1), irrespective of the identity of the central M^{IV} ion, and are characteristic of a neutral (bpy^0) molecule.[4a]

Unsurprisingly, the same holds true for *cis*-$[Si^{IV}(bpy^0)_2Cl_2]^{2+}$ (S = 0), with both the experimental and the geometry optimized structures containing two *N,N′*-coordinated (bpy^0) ligands, and the Si atom possessing a +IV oxidation state. Calculation of the hypothetical two-electron reduced congener $[Si(bpy)_2Cl_2]^0$ unambiguously shows that the two additional electrons are located in bpy-centered SOMOs (Figure 3), which yields the electronic structure description $[Si^{IV}(bpy^{\bullet})_2Cl_2]^0$. Structurally, this manifests as a respective shortening and elongation of the $C_{py}-C_{py}$ and C−N bonds to distances very similar to those determined by X-ray crystallography for alkali metal salts of the $(bpy^{\bullet})^-$ π-radical anion (Table 1).[4b]

Geometry optimization for the hypothetical Ge analogues, $[Ge(bpy)_2Cl_2]^n$ (n = 2+, 0), yields similar conclusions. More specifically, the octahedral dication possesses a *cis*-$[Ge^{IV}(bpy^0)_2Cl_2]^{2+}$ (S = 0) ground state containing a Ge^{IV} ion, two neutral (bpy^0) ligands and two *cis*-coordinated chloride ions. Addition of two electrons to give the neutral octahedral species $[Ge^{IV}(bpy^{\bullet})_2Cl_2]^0$ (S = 0) is again bpy-centered, so two π-radical $(bpy^{\bullet})^-$ anions are formed and Ge retains its +4 oxidation state.

Interestingly, while hypothetical $[Sn(bpy^0)_2Cl_2]^{2+}$ (S = 0) is computationally stable, this is not the case for its two electron reduced neutral form. Geometry optimization of $[Sn(bpy)_2Cl_2]^0$ converged not to an octahedral structure, but led effectively to dissociation of two (bpy^0) molecules and formation of a gas phase $Sn^{II}Cl_2$ molecule. Similarly, whereas hypothetical $[Pb(bpy)_2Cl_2]^0$ is not stable in silico, with geometry optimization resulting in formation of $Pb^{II}Cl_2$ and two uncoordinated (bpy^0) molecules, the corresponding octahedral dication *cis*-$[Pb^{IV}(bpy^0)_2Cl_2]^{2+}$ is computationally stable. The latter is a rare example of a Pb^{IV} compound (Pb^{II} is the dominant oxidation state). Of interest in this regard is the recent report of the synthesis and structural characterization of the bpy-containing octahedral Pb^{IV} complex $[Pb^{IV}(bpy^0)(Ph)_2Cl_2]^0$, in which the two phenylate anions are coordinated *trans* to one another and the *N,N′*-coordinated bpy ligand possesses structural parameters indicative of a (bpy^0) oxidation level ($C_{py}-C_{py}$ = 1.487 Å; average intrachelate C−N = 1.350 Å).[32]

The series of neutral $[M(bpy)Cl_2]^0$ (S = 0) compounds (M = Si, Ge, Sn, and Pb) are interesting because, in principle, the two limiting electronic structures $[M^{IV}(bpy^{2-})Cl_2]^0$ and $[M^{II}(bpy^0)Cl_2]^0$ are equally plausible. As detailed above, the silicon species exhibits a tetrahedral geometry with two bound chloride ions and an *N,N′*-coordinated dianionic $(bpy^{2-})^{2-}$ ligand, which displays near identical $C_{py}-C_{py}$ and C−N bond distances to alkali metal salts of this dianion. Thus, the central silicon ion is tetravalent and the electronic structure is $[Si^{IV}(bpy^{2-})Cl_2]^0$. It should be pointed out that the calculated Si−N bond length of 1.721 Å is very similar to the value of 1.701 Å observed in the X-ray structure of $[Si(NHCH_3)_4]^0$[29] and corresponds to a Si−N single bond without appreciable Si−N double bond character, which implies minimal π-donation by the amido nitrogen atoms.[33] Additionally, the calculated Si−Cl bond length of 2.061 Å is in close agreement with the average bond length of 2.008 Å in solid $SiCl_4$.[24]

In contrast, the corresponding Ge, Sn, and Pb $[M(bpy)Cl_2]^0$ compounds are all calculated to contain a neutral *N,N′*-coordinated (bpy^0) ligand, which renders the central ions divalent. In all three cases, two geometry optimized structures could be located, with the Cl−M−Cl unit being bent (*cis*-isomer) in one and nearly linear (*trans*-isomer) in the other. The *cis*-isomer was calculated to be the global energy minimum for all three, and whereas this conforms to the experimentally observed structure in the Sn case,[26] the X-ray structure of the Ge compound possesses a *trans* geometry.[25] In summary, in the $[M(bpy)Cl_2]^0$ series the Ge, Sn, and Pb compounds all possess a divalent central ion, and only the Si species is tetravalent.

The electronic structures of the series $[M(bpy)_2]^0$ and $[M(bpy)_2]^{2+}$ (M = C, Si, Ge, Sn, Pb) display a number of interesting trends. The calculated structures of the molecule $[C^{IV}(bpy^{2-})_2]^0$ (S = 0), which has yet to be reported, and its crystallographically characterized silicon analogue $[Si^{IV}(bpy^{2-})_2]^0$ (S = 0) are both tetrahedral and exhibit bpy

dx.doi.org/10.1021/ic401375a | Inorg. Chem. 2013, 52, 10067−10079

structural parameters characteristic of $(bpy^{2-})^{2-}$ dianions. In addition, the C−N and Si−N bond lengths in these compounds are comparable to those in the crystal structures of $[C^{IV}(N(CH_3)_2)_4]^0$[28b] and $[Si^{IV}(NHCH_3)_4]^0$,[29] and are typical of single bonds. On the basis of the aforementioned data, $[C^{IV}(bpy^{2-})_2]^0$ and $[Si^{IV}(bpy^{2-})_2]^0$ are perhaps best thought of as coordination compounds with a central C^{4+} and Si^{4+} ion.[34] This notion is supported by the minimal contribution of the central tetravalent atom to the two degenerate bpy-centered HOMOs observed in both cases. The same can also be said of the corresponding hypothetical dications $[C^{IV}(bpy^{\bullet})_2]^{2+}$ and $[Si^{IV}(bpy^{\bullet})_2]^{2+}$, which are most correctly described as being diradicals with triplet ground states. The aforementioned unpaired electrons reside in bpy-centered π^*-orbitals (the Mulliken spin population analysis reveals that the central Si and C atoms bear <0.04 unpaired spins), and the C−N and Si−N bonds are once again single bonds.

It is worthy of note that Norman and Russell et al.[35] have recently reported X-ray crystal structures and DFT calculations for $[B^{III}(bpy^{\bullet})Cl_2]^0$ (S = 1/2) and $[B^{III}(bpy^0)Cl_2]Cl$ (S = 0). Based upon the experimentally observed $C_{py}-C_{py}$ and C−N bond distances, the oxidation states of the bpy ligands can be unambiguously assigned as $(bpy^{\bullet})^-$ in the former case and (bpy^0) in the latter. Hence, the central boron ion is trivalent in both compounds. These electronic structure assignments were supported by DFT calculations, with the Mulliken spin density analysis for the neutral compound placing ∼95% of the unpaired spin on the bpy ligand and only 0.15% on the boron atom. Electron paramagnetic resonance (EPR) spectroscopy corroborates this picture. In addition, the diamagnetic compound $[B^{III}(bpy^0)_2]I_3$,[36] and the paramagnetic species $[B^{III}(bpy^{2-})(bpy^{\bullet})]^0$ (S = 1/2)[37] and $[B^{III}(Ph)_2(bpy^{\bullet})]^0$ (S = 1/2)[38] have been synthesized, but have yet to be structurally characterized. The presence of $(bpy^{\bullet})^-$ radical anions in the latter set of compounds was confirmed by EPR spectroscopy.

The electron transfer series $[Si(bpy)_3]^n$ (n = 1+, 0, 1−, 2−) all display octahedral geometry optimized structures, whose average Si−N bond distances were calculated to fall in the narrow range 1.904−1.914 Å (Figure 14) and are consistent with single bonds in all cases. Their electronic structures are best described as $[Si^{IV}(bpy^{\bullet})_3]^+$ (S = 1/2), $[Si^{IV}(bpy^{\bullet})_2(bpy^{2-})]^0$ (S = 0), $[Si^{IV}(bpy^{\bullet})(bpy^{2-})_2]^-$ (S = 1/2), and $[Si^{IV}(bpy^{2-})_3]^{2-}$ (S = 0). Thus, the successive one electron reductions associated with moving from the monocation to the dianion are all bpy-centered, and the Si ion retains a +IV oxidation state throughout. The stepwise reduction of the bpy ligands manifests as a linear decrease of the average $C_{py}-C_{py}$ bond length, and conversely a linear increase of the average intrachelate C−N bond length dianion (Figure 14). Such behavior has been observed in multiple instances for tris(bipyridine) complexes of transition metal ions.[9]

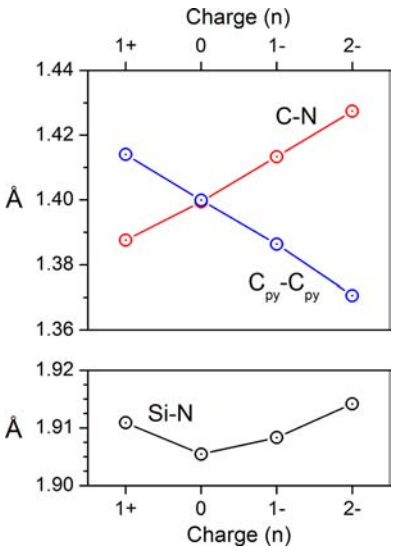

Figure 14. Plot of the average calculated $C_{py}-C_{py}$, C−N, and Si−N bond lengths versus charge (n) for the series $[Si(bpy)_3]^n$ (n = 1+, 0, 1−, 2−).

Interestingly, whereas the $[M(bpy)_3]^0$ compounds of Ge and Sn are also computationally stable and give S = 0 BS(1,1) $[M^{IV}(bpy^{\bullet})_2(bpy^{2-})]^0$ ground state electronic structures, geometry optimizations for $[Pb(bpy)_3]^0$ always proceed with dissociation of at least one (bpy^0) ligand. Indeed, the latter converge to the same Pb-containing species as those obtained for the corresponding calculations for the bischelate compound $[Pb(bpy)_2]^0$. The computational instability of $[Pb(bpy)_3]^0$ reflects the inherent instability of the +IV oxidation state for Pb and suggests that, unlike its Ge and Sn analogues, this compound is not likely to be synthetically accessible.

In summary, this DFT study has allowed assignment of ground state electronic structures of several experimentally known "low-valent" silicon bpy compounds, plus those of a series of closely related hypothetical species of the other group 14 elements. The computational stability/instability of the latter has allowed identification of several intriguing non-innocent main group species that appear to be synthetically viable. It should be noted that although a small number of true Si^{II} and Si^0 compounds have now been prepared,[39] all the "low-valent" Si compounds in this study are correctly described as containing Si^{IV} and reduced bpy ligands. Additionally, as might be expected, descending group 14 leads to enhanced stability of the divalent state, which is associated with a stereochemically active electron pair and results in heavily distorted structures. Lastly and most crucially, many of the core observations that we[9] and others[10] have made regarding bpy noninnocence in transition metal complexes are equally applicable to p-block chemistry in cases where the elements in question are significantly less electronegative than the N-donors of bpy.

■ ASSOCIATED CONTENT

Supporting Information

Further information regarding the DFT calculations, including tables of atomic coordinates, bond distances, and energies, plus additional Mulliken spin density plots and qualitative frontier molecular orbital diagrams. This material is available free of charge via the Internet at http://pubs.acs.org.

■ AUTHOR INFORMATION

Corresponding Author

*E-mail: karl.wieghardt@cec.mpg.de.

Notes

The authors declare no competing financial interest.

■ ACKNOWLEDGMENTS

J.E. thanks the Max Planck Society for financial support.

DEDICATION

We dedicate this paper to Professor Bernt Krebs on the occasion of his 75th birthday.

REFERENCES

(1) Herzog, S.; Krebs, F. *Naturwissenschaften* **1963**, *50*, 330.
(2) Wulf, E.; Herzog, S. *Z. Anorg. Allg. Chem.* **1972**, *387*, 81.
(3) Morancho, R.; Pouvreau, P.; Constant, G.; Jaud, J.; Galy, J. *J. Organomet. Chem.* **1979**, *166*, 329.
(4) Throughout this paper we use the abbreviation bpy in a generic sense without specifying the oxidation level of the 2,2′-bipyridine ligand. When specificying the oxidation level, (bpy^0) is used for the neutral ligand, $(bpy^{\bullet})^-$ for the π-radical anion, and $(bpy^{2-})^{2-}$ for the diamagnetic dianion (see Scheme 1). Crystal structures of "uncoordinated" (bpy^0) and alkaline salts of $(bpy^{\bullet})^-$ and $(bpy^{2-})^{2-}$ have been reported: (a) (bpy^0): Chisholm, M. M.; Huffmann, J. C.; Rothwell, I. P.; Bradley, P. G.; Kress, N.; Woodruff, W. M. *J. Am. Chem. Soc.* **1981**, *103*, 4945. (b) $(bpy^{\bullet})^-$: Gore-Randall, E.; Irwin, M.; Denning, M. S.; Goicoechea, J. M. *Inorg. Chem.* **2009**, *48*, 8304. (c) $(bpy^{2-})^{2-}$: Bock, H.; Lehn, J.-M.; Pauls, J.; Holl, S.; Krenzel, V. *Angew. Chem., Int. Ed.* **1999**, *38*, 952.
(5) Herzog, S.; Zimmer, F. *Z. Chem.* **1967**, *7*, 396.
(6) Wannagat, U. *Angew. Chem.* **1957**, *69*, 516.
(7) Portius, P.; Filippou, A. C.; Schnakenburg, G.; Davis, M.; Wehrstedt, K.-D. *Angew. Chem., Int. Ed.* **2010**, *49*, 8013.
(8) Adley, A. D.; Bird, P. H.; Fraser, A. R.; Onyszchuk, M. *Inorg. Chem.* **1972**, *11*, 1402.
(9) (a) Scarborough, C. C.; Sproules, S.; Weyhermüller, T.; DeBeer, S.; Wieghardt, K. *Inorg. Chem.* **2011**, *50*, 12446. (b) Scarborough, C. C.; Sproules, S.; Doonan, C. J.; Hagen, K. S.; Weyhermüller, T.; Wieghardt, K. *Inorg. Chem.* **2012**, *51*, 6969. (c) England, J.; Scarborough, C. C.; Weyhermüller, T.; Sproules, S.; Wieghardt, K. *Eur. J. Inorg. Chem.* **2012**, 4605. (d) Wang, M.; England, J.; Weyhermüller, T.; Kokatam, S.-L.; Pollock, C. J.; DeBeer, S.; Shen, J.; Yap, G. P. A.; Theopold, K. H.; Wieghardt, K. *Inorg. Chem.* **2013**, *52*, 4472.
(10) Irwin, M.; Doyle, L. R.; Kramer, T.; Herchel, R.; McGrady, J. E.; Goicoechea, J. M. *Inorg. Chem.* **2012**, *51*, 12301.
(11) Neese, F. *Orca, an Ab Initio Density Functional and Semiempirical Electronic Structure Program Package*, version 2.8, revision 2287; Universität Bonn: Bonn, Germany, 2010.
(12) (a) Becke, A. D. *Phys. Rev. A* **1988**, *38*, 3098. (b) Becke, A. D. J. *Chem. Phys.* **1993**, *98*, 5648. (c) Lee, C. T.; Yang, W. T.; Parr, R .G. *Phys. Rev. B* **1988**, *37*, 785.
(13) (a) Weigend, F.; Ahlrichs, R. *Phys. Chem. Chem. Phys.* **2005**, *7*, 3297. (b) Schäfer, A.; Huber, C.; Ahlrichs, R. *J. Chem. Phys.* **1994**, *100*, 5829.
(14) (a) van Wuellen, C. *J. Chem. Phys.* **1998**, *109*, 392. (b) van Leuthe, E.; Baerends, E. J.; Snijders, J. G. *J. Chem. Phys.* **1993**, *99*, 4597. (c) van Lenthe, E.; Baerends, E. J.; Snijders, J. G. *J. Chem. Phys.* **1994**, *101*, 9783. (d) Pantazis, D. A.; Chen, X. Y.; Landis, C. R.; Neese, F. *J. Chem. Theory Comput.* **2008**, *4*, 908.
(15) (a) Eichkorn, K.; Weigend, F.; Treutler, O.; Ahlrichs, R. *Theor. Chem. Acc.* **1997**, *97*, 119. (b) Eichkorn, K.; Treutler, O.; Öhm, H.; Häser, M.; Ahlrichs, R. *Chem. Phys. Lett.* **1995**, *240*, 283. (c) Eichkorn, K.; Treutler, O.; Öhm, H.; Häser, M.; Ahlrichs, R. *Chem. Phys. Lett.* **1995**, *242*, 652.
(16) (a) Neese, F.; Wennmohs, F.; Hansen, A.; Becker, U. *Chem. Phys.* **2009**, *356*, 98. (b) Kossmann, S.; Neese, F. *Chem. Phys. Lett.* **2009**, *481*, 240. (c) Neese, F. *J .Comput. Chem.* **2003**, *24*, 1714.
(17) (a) Pulay, P. *Chem. Phys. Lett.* **1980**, *73*, 393. (b) Pulay, P. *J. Comput. Chem.* **1992**, *3*, 556.
(18) (a) Noodleman, L. *J. Chem. Phys.* **1981**, *74*, 5737. (b) Noodleman, L.; Norman, J. G.; Osborne, J. H.; Aizman, A.; Case, D. *J. Am. Chem. Soc.* **1985**, *107*, 3418. (c) Noodleman, L.; Davidson, E. R. *Chem. Phys.* **1986**, *109*, 131. (d) Noodleman, L.; Case, D. A.; Aizman, A. J. *J. Am. Chem. Soc.* **1988**, *110*, 1001. (e) Noodleman, L.; Peng, C. Y.; Case, D. A.; Monesca, J. M. *Coord. Chem. Rev.* **1995**, *144*, 199.
(19) Neese, F. *J. Phys. Chem. Solids* **2004**, *65*, 781.
(20) Pettersen, E. F.; Goddard, T. D.; Huang, C. C.; Couch, G. S.; Greenblatt, D. M.; Meng, E. C.; Ferrin, T. E. *J. Comput. Chem.* **2004**, *25*, 1605.
(21) (a) Hoppe, R.; Dähne, W. *Naturwissenschaften* **1962**, *49*, 254. (b) Bork, M.; Hoppe, R. *Z. Anorg. Allg. Chem.* **1996**, *622*, 1557.
(22) (a) Kummer, D.; Seshadri, T. *Z. Anorg. Allg. Chem.* **1977**, *428*, 129. (b) Hensen, K.; Meyr-Stein, R.; Rühl, S.; Bolte, M. *Acta Crystallogr., Sect. C* **2000**, *C56*, 607.
(23) (a) Soda, T.; Kitagawa, Y.; Onishi, T.; Takano, Y.; Shigeta, Y.; Nagao, H.; Yoshioka, Y.; Yamaguchi, K. *Chem. Phys. Lett.* **2000**, *319*, 223. (b) Yamaguchi, K.; Takahara, Y.; Fueno, T. In *Applied Quantum Chemistry*; Smith, V. H.; Ed.; Reidel: Dordrecht, The Netherlands, 1986; p 155.
(24) Zakharov, L. N.; Antipin, M. Yu.; Struchkov, Yu. T.; Gusev, A. V.; Gibin, A. M.; Zhernenkov, N. N. *Sov. Phys., Crystallogr.* **1986**, *31*, 99; (also: *Kristallografiya* **1986**, *31*, 171)..
(25) Cheng, F.; Dyke, J. M.; Ferrante, F.; Hector, A. L.; Levason, W.; Reid, G.; Webster, M.; Zhang, W. *Dalton Trans.* **2010**, *39*, 874.
(26) Archer, S. J.; Koch, K. R.; Schmitt, S. *Inorg. Chim. Acta* **1987**, *126*, 209.
(27) Bowmaker, G. A.; Harrowfield, J. M.; Miyamae, H.; Shand, T. M.; Skelton, B. W.; Soudi, A. A.; White, A. H. *Aust. J. Chem.* **1996**, *49*, 1089.
(28) (a) Tetra(pyrrolyl)methane: Müller, M.; Lork, E.; Mews, R. *Angew. Chem., Int. Ed.* **2001**, *40*, 1247. (b) $[C(NMe_2)_4]^0$: Jokisch, A.; Schier, A.; Schmidbaur, H. *Chem. Ber./Rec.* **1997**, *130*, 1739. (c) Tetrakis(3,5-dimethylpyrazolyl)methane: Benisvy, L.; Wanke, R.; Kuznetzov, M. L.; Guedes da Silva, M. F. C.; Pombeiro, A. J. L. *Tetrahedron* **2009**, *65*, 9218.
(29) Andersch, H.; Jansen, M. *Acta Crystallogr., Sect. C* **1990**, *46*, 1985.
(30) (a) $[Pb^{II}(bpy^0)_2](PF_6)_2$: Karlarkaraisamy, M.; Engehart, D. P.; Basa, P. N.; Sykes, A. G. *J. Coord. Chem.* **2010**, *63*, 2261. (b) $[Pb(bpy^0)_2][B_{12}H_{12}]$: Lagun, V. L.; Oriova, A. M.; Katser, S. B.; Sointsev, K. A.; Kuznetzov, N. T. *Koord. Khim. (Russ. Coord. Chem.)* **1994**, *20*, 431.
(31) Klamt, A.; Schüürmann, G. *J. Chem. Soc., Perkin Trans. 2* **1993**, 799.
(32) Casas, J. S.; Castellano, E. E.; Ellena, J.; Garcia-Tasende, M. S.; Sanchez, A.; Sordo, J.; Vidarte, M. J. *Main Group Met. Chem.* **2001**, *24*, 297.
(33) Albert, K.; Rösch, N. *Chem. Ber./Rec.* **1997**, *130*, 1745.
(34) Schmidbaur, H.; Schier, A. *Angew. Chem., Int. Ed.* **2013**, *52*, 176.
(35) Mansell, S. M.; Adams, C. J.; Bramham, G.; Haddow, M. F.; Kaim, W.; Norman, N. C.; McGrady, J. E.; Russell, C. A.; Udeen, S. J. *Chem. Commun.* **2010**, *46*, 5070.
(36) Bohl, R. D.; Galloway, G. L. *J. Inorg., Nucl. Chem.* **1971**, *33*, 885.
(37) Kuck, M. A.; Urry, G. *J. Am. Chem. Soc.* **1966**, *88*, 426.
(38) Kaim, W. *Chem. Ber.* **1981**, *114*, 3789.
(39) (a) Xiong, Y.; Yao, S.; Inoue, S.; Epping, J.-D.; Driess, M. *Angew. Chem., Int. Ed.* **2013**, *52* (28), 7147. (b) Mondal, K. C.; Roesky, H. W.; Schwarzer, M. C.; Frenking, G.; Niepötter, H.; Wolf, H.; Herbst-Irmer, R.; Stalke, D. *Angew. Chem., Int. Ed.* **2013**, *52*, 2963. (c) Wang, Y.; Xie, Y.; Wie, P.; King, R. B.; Schaefer, H. F.; Schleyer, P. v. R.; Robinson, G. H. *Science* **2008**, *321*, 1069. (d) Tonner, R.; Frenking, G. *Angew. Chem., Int. Ed.* **2007**, *46*, 8695. (e) Takagi, N.; Tonner, R.; Frenking, G. *Chem.—Eur. J.* **2012**, *18*, 1772.